ChemPubSoc Europe

DOI: 10.1002/ejoc.201600296

EurJOC European Journal of Organic Chemistry

Full Paper

Organocatalysis

An Atropisomerically Enforced Phosphoric Acid for Organocatalytic Asymmetric Reactions

Luca Bernardi,[a] Giada Bolzoni,[a] Mariafrancesca Fochi,[a] Michele Mancinelli,[a] and Andrea Mazzanti*[a]

Dedicated to Professor Achille Umani Ronchi on the occasion of his 80th birthday

Abstract: Three BINOL-derived phosphoric acids exhibiting atropisomerism in the 3,3′-positions were obtained by Suzuki coupling reaction. The diastereomeric mixture was resolved by HPLC. Structural assignment was achieved by NOE-NMR analysis and by TD-DFT simulation of the electronic circular dichroism (ECD) spectra. The three atropisomeric catalysts were tested in three enantioselective reactions, comparing their ability to induce enantioselectivity with related, well-known, phosphoric acid structures. All three catalysts were competent in promoting the reactions, rendering excellent enantioselectivity (98 % *ee*) in one case. The atropisomeric features at the 3,3′-position were indeed found to influence the outcome of the reaction, demonstrating the potential of atropisomeric conformational control at the 3,3′-position of the BINOL core in the rationalization of catalyst performances and in the design of new efficient structures.

Introduction

The search for new atropisomeric systems and the related conformational analysis is still a broad field of research. On the other hand, the development of new chiral Brønsted acids, and in particular phosphoric acids,[1] is an area of great interest for organocatalysis. Combining these two spheres of research, we speculated on the preparation of a chiral Brønsted acid catalyst with additional atropisomeric features. Many of the phosphoric acids synthesized and applied so far derive from structural modifications of BINOL featuring aryl substituents at the 3- and 3′-positions. The well-known and high-performing derivatives **1**[2] and **2**[3] are highly congested systems. Although the rotation around the aryl–aryl bond is sterically hindered, it does not produce additional chiral axes because of the local C_{2v} symmetry of tris-2,4,6-(isopropyl)phenyl and 9-anthracenyl moieties (Figure 1). Dissymmetric but less hindered substituents such as 1-naphthyl in catalyst **3**[4] give instead rapid interconversion at ambient temperature, precluding the isolation of the single atropisomers. Consequently, to develop atropisomerism, the substituents linked to positions 3 and 3′ of the BINOL scaffold should be both non-C_2-symmetric at their point of insertion and sufficiently hindered to prevent free rotation.[5] Our attention fell on 2-methylnaphthalene, which can be introduced by using a standard Suzuki–Miyaura reaction. The resulting phosphoric acid catalyst **4** features flat aromatic rings at the 3,3′-positions, reminiscent of the 1-naphthyl derivative **3**. However, the arrangement of these rings and of the methyl substituents

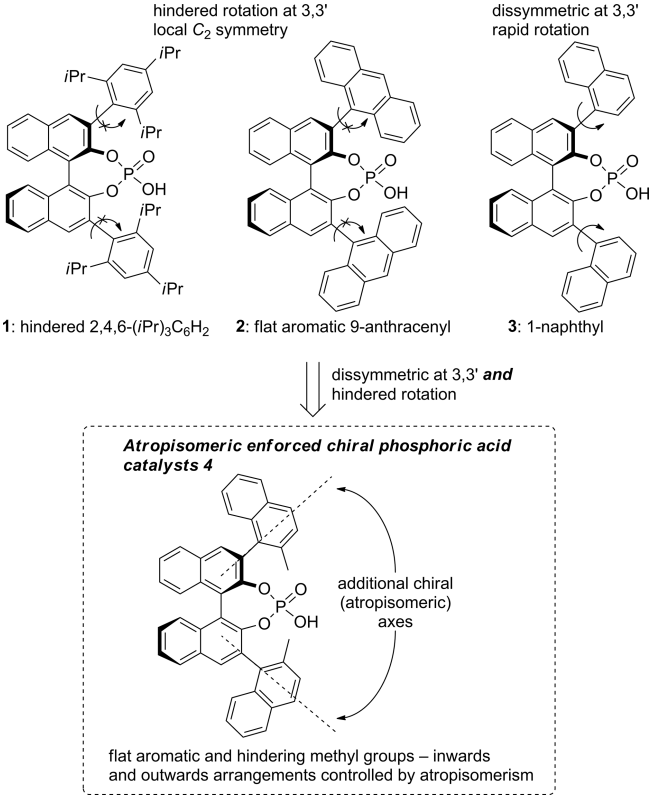

Figure 1. Atropisomerically enforced chiral phosphoric acid catalysts **4**.

[a] *Department of Industrial Chemistry "Toso Montanari", University of Bologna,*
Viale Risorgimento 4, 40136 Bologna, Italy
E-mail: andrea.mazzanti@unibo.it
https://www.unibo.it/sitoweb/andrea.mazzanti

Supporting information for this article is available on the WWW under http://dx.doi.org/10.1002/ejoc.201600296.

in phosphoric acid **4** is "frozen"; catalysts featuring these groups pointing inwards and outwards relative to the catalophoric phosphoric acid can be isolated and tested for catalytic performance.

The local symmetry of the 2-methylnaphthyl moiety adds two additional stereogenic axes to the BINOL scaffold when the aryl–aryl rotation is frozen. The steric constrains of the 2-methylnaphthyl ring mean that the rotational barrier should be sufficiently high to produce atropisomers that are stable at and above room temperature. From the point of view of aryl–aryl rotation, the system is indeed a trisubstituted biaryl system, and, compared with the BINOL scaffold (a tetrasubstituted biaryl system), the rotational barrier of 2-methylnaphthyl should be smaller, thus making the thermal interconversion of the atropisomers through 2-methylnaphthyl rotation conceivable, leaving unchanged the conformational chirality of BINOL.

From a stereochemical point of view, the presence of two additional stereogenic axes should produce four diastereoisomers. However, the two stereogenic axes between BINOL and 2-methylnaphthalene are mutually related by the C_2 axis of the BINOL, thus only three diastereoisomers are generated (Figure 2). They can be conveniently described by using the *M*/*P* terminology[6] as (1) ***M***,*M*,*M*, (2) ***M***,*P*,*P*, and (3) ***M***,*P*,*M*≡***M***,*M*,*P* (hereafter the bold descriptor is related to the stereogenic axis of enantiopure *M*-BINOL).

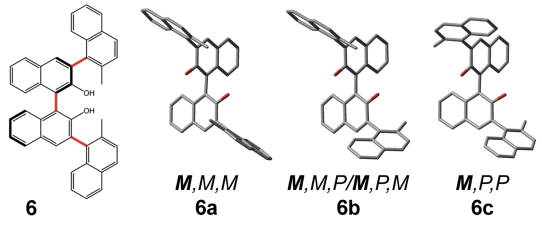

Figure 2. The three available diastereoisomers of the binaphthol precursor **6**, optimized at the B3LYP/6-31G(d) level. Hydrogen atoms are omitted for clarity.

Table 1. Summary of the relative conformational energies of the three diastereoisomers of **4** (relative energies in kcal/mol), calculated at the B3LYP/6-31G(d) level of theory.

Diastereoisomer	Conf. 1	Conf. 2	Conf. 3
M,*P*,*P*	0.83	1.10	0.06
M,*M*,*P*	0.70	0.88	0.00
M,*M*,*M*	0.71	0.68	0.01

Results and Discussion

Before undertaking the synthetic preparation, computational studies were performed to understand the relative stability of the conformers outlined in Figure 2, and to evaluate the theoretical rotational barrier to assess a priori whether the conditions for atropisomerism can be met. Binaphthol **6** (i.e., the precursor of the target phosphoric acid **4**, see Figure 2) was selected for computational analysis. The ground states for the three conformational diastereoisomers of **6** were optimized at the B3LYP/6-31G(d) level. The presence of the two OH groups in close proximity meant that more than one energy minimum was found for each diastereoisomer because of the different disposition of the two hydroxyl groups. These may assume three available dispositions (see the Supporting Information for details), the energies of which are summarized in Table 1.

Within each diastereoisomer, the most stable geometry corresponds to the same disposition of the OH pointing towards each other. Although the ***M***,*M*,*P* diastereoisomer is calculated to be the most stable, the relative energies are very similar and a reliable prediction cannot be inferred. On the other hand, the very similar energies forecast an equilibrium population in which all three diastereoisomers should be populated with a similar ratio.

Given the symmetry of the system, the rotational path of the 2-methylnaphthyl moieties may be modeled for only one of them, the other being related by symmetry. Two different transition states have to be considered for the interconversion between the three atropisomeric structures. The first transition state (TS) corresponds to the crossing of the 2-methyl group over the OH (TS1, Figure 3, left), whereas the second TS corresponds to a rotation of the 2-methyl over the hydrogen in position 4 of the BINOL (TS2, Figure 3, right). DFT calculations run at the B3LYP/6-31G(d) level suggest that TS1 has a lower energy with respect to TS2 (29.4 and 31.0 kcal/mol, respectively). In both cases, however, the suggested energy values should be sufficiently high to develop stable atropisomers at and above room temperature.

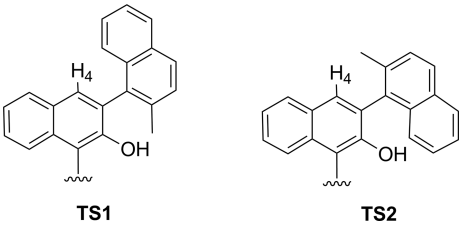

Figure 3. The two available transition states for diasteromerization due to the 2-methylnaphthyl rotation.

Preparation

Compound **5** was obtained by using two different approaches (Scheme 1), both based on the Suzuki–Miyaura coupling reaction starting from (*M*)-2,2′-dimethoxy-1,1′-binaphthalene, which was treated with *n*Buli/TMEDA and then converted into (*M*)-(2,2′-dimethoxy-[1,1′-binaphthalene]-3,3′-diyl)diboronic acid or (*M*)-3,3′-diiodo-2,2′-dimethoxy-1,1′-binaphthalene by reaction with trimethylborate or iodine. The two intermediates were then reacted with 2-bromo-1-methylnaphthalene (route A) or 2-methylnaphthylboronic acid (route B) by using $Pd(PPh_3)_4$ as catalyst and $Ba(OH)_2$ as the base in a dioxane/water (3:1) mixture.

Good conversion by using the first procedure required the use a large excess of the aromatic halide (10 equiv.) to reduce the amount of byproducts deriving from monocoupling followed by dehalogenation of the intermediate. The coupling reaction occurred in about 18 h at 70 °C with 50–55 % yield. As

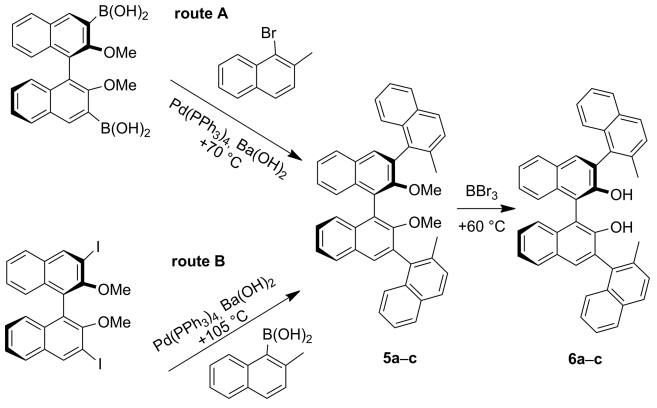

Scheme 1.

a variation of the previous method, the coupling reaction between (*M*)-3,3′-diiodo-2,2′-dimethoxy-1,1′-binaphthalene and 2-methylnaphthyl-boronic acid (4 equiv.) was conducted at reflux (ca. 105 °C) for 6 h while maintaining a constant flow of nitrogen, with a 45–50 % yield in compound **5**.

The ^{1}H NMR spectrum of the crude material from the first reaction showed four singlet signals in the methyl region, as well as for the OMe signals (see Figure 4). Within each set of signals, two had the same intensity whereas the remaining two signals had different intensities (54:19:19:8 ratio). This is in agreement with the presence of the three diastereoisomers **5a**–**c**. The two C_2-symmetric diastereoisomers (***M***,*M*,*M* and ***M***,*P*,*P*) display half of the signals both in the ^{1}H and ^{13}C NMR spectra. In contrast, the asymmetric diastereoisomer exhibits different signals for all hydrogen atoms because of its C_1 symmetry. It was therefore straightforward to assign the ***M***,*M*,*P* diastereoisomer **5b** to the diastereoisomer showing two methyl signals with the very same intensity.

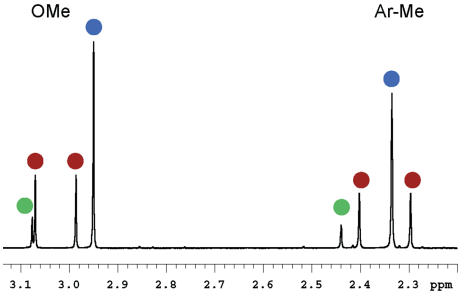

Figure 4. ^{1}H NMR spectrum of the diastereomeric mixture of **5** (25 °C, 600 MHz in $CDCl_3$). The red dots indicate the C_1-symmetric diastereoisomer (***M***,*M*,*P*), whereas blue and green dots mark the two C_2-symmetric diastereoisomers.

Several separation tests using reverse-phase C18 columns on HPLC apparatus showed that the separation of the atropisomeric mixture **5** was not achievable under such conditions. The protecting OMe groups were therefore removed at this stage to increase the polarity of the compounds. The reaction with BBr_3 was conducted below 60 °C to avoid thermal equilibration due to 2-methylnaphthyl rotation. Under these conditions, good conversion in binaphthols **6a**–**c** was obtained. HPLC analysis on C18 stationary phase now showed three well-separated peaks with the same molecular weight, corresponding to the three diastereoisomers of **6**. The HPLC traces reported in Figure 5 are relative to the pre-purified crude material of the deprotected binaphthols **6a**–**c**. The different ratio observed for the two traces (54:38:8 vs. 46:42:12) suggests either that partial equilibration occurred during the coupling reaction at higher temperatures, or a different stereochemical outcome of the Suzuki coupling depending on the reagents combination.

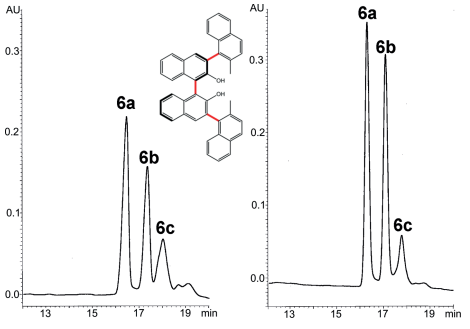

Figure 5. HPLC chromatograms of compound **6**. Right: route A. Left: route B (C18 column, see Exp. Sect. for details).

To gain more information about the thermal stability of the two stereogenic axes, the first chromatographic peak was collected from a semipreparative C18 column and the compound was dissolved in $C_2D_2Cl_4$ and kept at 100 °C in an oil bath. NMR spectra were then collected at defined times to monitor the conversion of the single diastereoisomer to the thermodynamic mixture. NMR spectra confirmed that the first eluted peak corresponds to one of the two C_2-symmetric atropisomers (see next section for the assignment), and a thermodynamic ratio of 25:50:25 was reached after 10 d at 100 °C (see the Supporting Information).

Degradation byproducts were not observed during any of the procedures. Given the complexity of the full kinetic treatment of an equilibrium reaction with three exchanging species, the reaction rate for interconversion of the pure compound into the thermodynamic mixture was derived by using the kinetic data at the beginning of the reaction with the simpler initial rate approach. This method yielded a rate constant of 2.7×10^{-6} s^{-1} at 100 °C, corresponding to $\Delta G^{\neq}$ = 31.5 kcal/mol. This barrier corresponds to a lifetime of more than 400 years at ambient temperature, and it confirms the reliability of preliminary calculations. At the same time, the barrier is much lower than that of BINOL (37 kcal/mol),[7] so the central stereogenic axis can be preserved during thermal diastereoisomerization.

The ratio observed after thermal equilibration is rather different from that observed in the crude reaction product. This suggests that enantiopure *M*-BINOL drives both the first and the second coupling reactions mainly towards one of the three diastereoisomers,[8] and the coupling conditions (6 h at 105 °C) cannot bring the system to the thermodynamic equilibrium. This phenomenon can be confirmed by the more unbalanced ratio obtained when lower temperatures (70 °C, see first synthetic route) were used during the cross-coupling reaction. The reaction can therefore provide a larger amount of the first eluted diastereoisomer if the separation is carried out just after

the reaction, or a larger amount of the second eluted atropisomer if the purification is performed after thermal equilibration.

Structural Assignment

Whereas the assignment of the C_1-symmetric ***M***,*M*,*P* was straightforward, NOE experiments were performed on the two C_2-symmetric diastereoisomers to assign their configuration. In both compounds, some NOE effects can act as control signals while additional NOEs can be used for diagnostic purposes. On saturation of the 2-methyl signal, the H-4 on BINOL and H-3′ on naphthalene must experience NOE enhancement due to their proximity with the 2-methyl group in both diastereoisomers. In contrast, in the case of the ***M***,*P*,*P* diastereoisomer (for which the two methyl groups point outward), an additional enhancement should also be observed for H-8; that is, the *peri* hydrogen of the second ring of BINOL. Although both methyl signals are simultaneously saturated because of their chemical shift equivalence, the enhancement on H-8 remains diagnostic because this hydrogen is far from the 2-methyl within the *same* naphthol ring, but it is only 3.6 Å apart from the methyl bound to the naphthalene of the *other* naphthol ring of BINOL (red arrow in Figure 6).

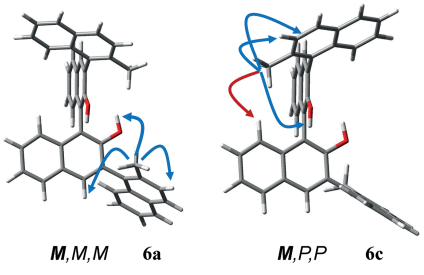

Figure 6. 3D structures of the two C_2-symmetric diastereoisomers of **6**. Blue arrows indicate control NOE, whereas the red arrow indicates the diagnostic NOE.

The experimental NOE spectra[9] shown in Figure 7 confirmed that only in one case was the signal of H-8 observed on saturation of the methyl signals, thus confirming the validity of the theoretical approach.

These results allowed the assignment of the ***M***,*M*,*M* configuration to the first eluted diastereoisomer **6a**, and the ***M***,*P*,*P* configuration to the third eluted diastereoisomer **6c**, with the ***M***,*P*,*M*/***M***,*M*,*P* diastereoisomer **6b** being the second eluted compound. Electronic circular dichroism (ECD) spectra of the three diastereoisomers were acquired in acetonitrile to further support the assignment based on NOE spectra (see Figure 8). For the comprehension of the ECD spectra it should be taken into account that they are dominated by the exciton couplings arising from any pair of bonded naphthalenes. As a second note, the exciton couplings are generated by the two dipoles on the long axis of the naphthalenes; thus, they are related to the sign of the dihedral angle starting from the quaternary carbon in position 9 of the naphthalene, independent of whether this has higher or lower CIP priority with respect to the carbon in position 2.

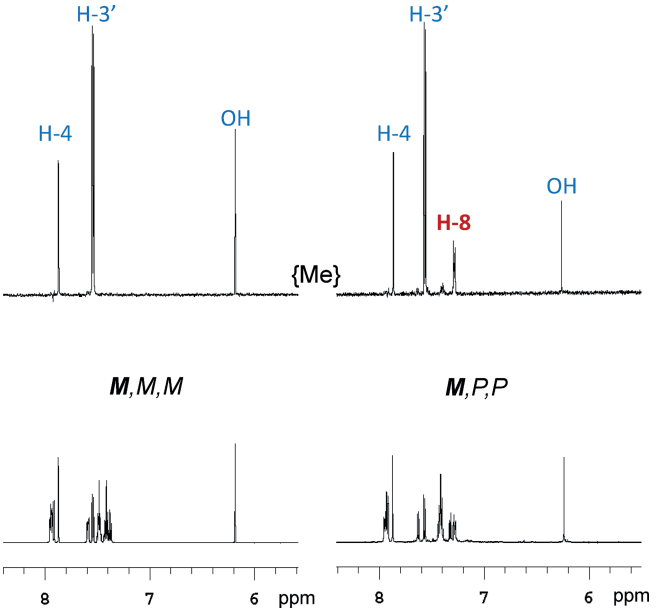

Figure 7. DPFGSE-NOE spectra of the two C_2 symmetric diastereoisomers of **6** on saturation of the 2-methyl signal.

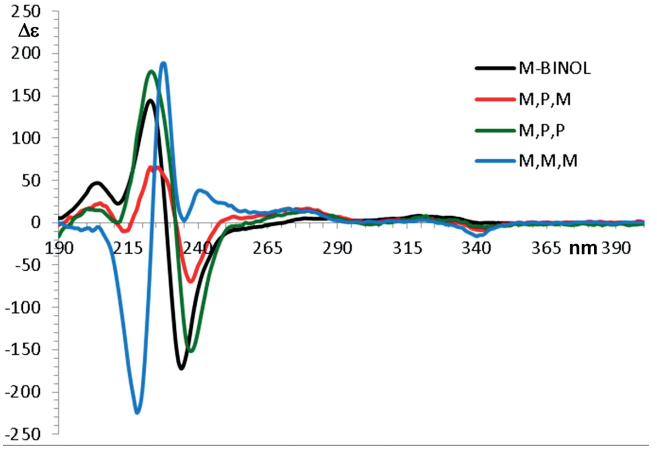

Figure 8. ECD spectra of *M*-BINOL and of the three diastereoisomers of **6**, taken in acetonitrile.

In the most simple case of the ***M***,*P*,*M*/***M***,*M*,*P* atropisomer **6b**, the two 2-methylnaphthalenes have opposite dihedral angle with each naphthol ring of *M*-BINOL, and their exciton couplings mainly compensate themselves. The resulting ECD spectrum is therefore due to the *M*-BINOL exciton coupling, yielding an ECD trace very similar in terms of shape and intensity to that of *M*-BINOL itself (red line in Figure 8).

When the two C_2-symmetric diastereoisomers are considered, the exciton coupling of two external stereogenic axes are governed by the $C9_{Naph}$–$C1_{Naph}$–$C3_{BINOL}$–$C2_{BINOL}$ dihedral angle, whereas the central stereogenic axis of BINOL is defined by the C2′–C1′–C1–C2 dihedral angle. As a consequence, when the two naphthol rings have negative dihedral angle (*M*-BINOL configuration), the corresponding disposition of each naphthol ring with 2-methylnaphthalene switches to a *P* configuration. The ECD spectra of the two symmetric atropisomers should be con-

sidered within this framework. In the case of the ***M*,*M*,*M*** diastereoisomer **6a**, the two exciton couplings due to the external stereogenic axes are positive and opposite to that of the central axis, thus the ECD spectrum yields a positive exciton coupling due to the subtraction of the negative *M*-BINOL exciton from the two positive excitons of 2-methylnaphthalene (blue trace in Figure 8). When the ***M*,*P*,*P*** atropisomer **6c** is considered, the three dihedral angles are all negative and the excitons sum up, yielding a strong negative coupling.

Given that the three stereogenic axes are not exactly equivalent and the external dihedral angles could be different from that of *M*-BINOL, the previous considerations could be thwarted by the different dipole disposition and absorption wavelength. To confirm the assignment, we performed TD-DFT simulations of the ECD spectra.[10] In the present case, the molecules are very rigid and only one conformation must be considered.[11] The electronic excitation energies and rotational strengths were calculated in the gas phase by using the geometries optimized at the B3LYP/6-31G(d) level and using TD-DFT with four different functionals to explore whether different theoretical models provide different shapes of the simulated spectra. Simulations were performed by using the hybrid functionals BH&HLYP[12] and M06-2X,[13] the long-range correlated ωB97XD,[14] which includes dispersion, and CAM-B3LYP,[15] which includes long-range correction. All the simulations employed the 6-311+G(d,p) basis set (Figure 9). In all cases, the ECD simulations reproduce well the experimental spectra, thus confirming the assignment made based on NMR spectroscopy.

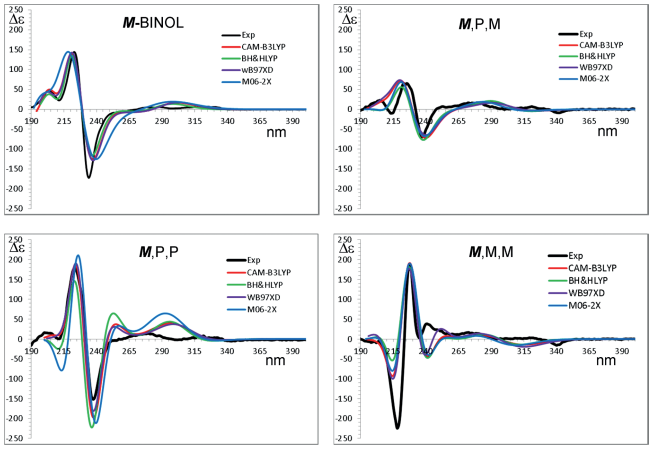

Figure 9. ECD spectra and TD-DFT simulations for *M*-BINOL and of the three diastereoisomers of compound **6**. The black trace corresponds to the experimental spectrum in acetonitrile. The four colored lines are the TD-DFT simulations obtained with four different functionals and the 6-311++G(2d,p) basis set.

Once separated and identified, compounds **6a**–**c** needed to be converted into phosphoric acids **4a**–**c** to determine whether they could be successfully applied in asymmetric synthesis with good performance. Reported synthetic routes to obtain catalysts **1**[16] and **2**[17] employ too drastic reaction temperatures (ca. 100 °C for more than 24 h), at which the thermal stability of the two stereogenic axes is not complete. It was therefore necessary to use a synthetic method that operates at a temperature not exceeding 60 °C. By following a reported procedure,[18] compounds **6a**–**c** were treated with a concentrated solution of $POCl_3$ in anhydrous pyridine under nitrogen flow. The reaction was carried out at 60 °C until disappearance of the starting compounds (16–20 h). The final phosphoric acids **4a**–**c** were acidified with concentrated HCl at ambient temperature to remove all the salts, and fully characterized by means of ^1H, ^{13}C, and ^{13}P NMR spectroscopy.

Catalytic Tests

Having at hand the three atropisomeric forms of the phosphoric acids **4a**–**c**, we were eager to test their performances in promoting catalytic enantioselective reactions. Catalyst **4a** features a C_2-symmetry with the methyl groups pointing towards the catalytic center, which is reminiscent of the steric hindrance offered by the large 2,6-isopropyl groups of catalyst **1** (Figure 1). In catalyst **4c**, which is also C_2-symmetric, the methyl groups point outwards; the active center is thus closer to the flat aromatic rings of the naphthalene units. Such arrangement looks more related to the 9-anthracenyl-substituted catalyst **2** (Figure 1). Catalyst **4b** is not C_2-symmetric; one methyl group points inwards, the second one outwards. Based on our experience in phosphoric acid catalysis[19] and considering these structural features, we initially selected two known asymmetric transformations wherein catalysts **1** and **2** show contrasting behaviors, and which we thought useful to compare the catalytic performances of **4a**–**c** with these phosphoric acid catalysts. We also included the "non-frozen" 1-naphthyl-substituted catalyst **3** for this comparison.

We first studied the Povarov reaction[20] between the *N*-4-methoxyphenyl aldimine **7** and 2-vinylindole **8** (Table 2).[19a] In this reaction, the highly hindered catalyst **1** affords very good enantioselectivity (entry 1), whereas the 9-anthracenyl derivative **2**, bearing flat substituents, is less efficient (entry 2). The 1-naphthyl-substituted catalyst **3** affords intermediate results (entry 3).

Table 2. Povarov reaction between imine **7** and 2-vinylindole **8** catalyzed by **4a**–**c**, and comparison with catalysts **1**–**3**.[a]

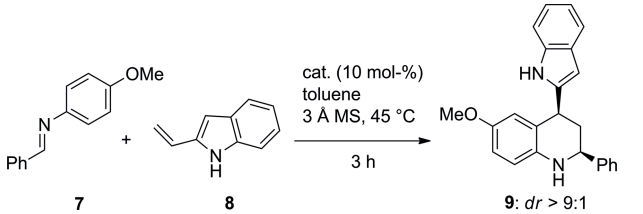

7 **8** **9**: *dr* > 9:1

Entry	Catalyst	Conversion[b] [%]	*ee*[c] [%]
1[d]	*ent*-**1**	>90	98
2[d,e]	*ent*-**2**	88	66
3	**3**	65	81
4	**4a**	72	91
5	**4b**	68	77
6	**4c**	61	84

[a] Reaction conditions: imine **7** (0.025 mmol), catalyst **4** (0.0025 mmol, 10 mol-%), vinylindole **8** (0.0275 mmol), 3 Å MS, toluene, 45 °C, 3 h. [b] Determined by ^1H NMR spectroscopic analysis after a plug on silica gel and evaporation of the solvents. [c] Determined by CSP-HPLC analysis. [d] Refers to *ent*-**9**. Data taken from ref.[19a] [e] Reaction performed at room temp. for 72 h, in the absence of MS.

We were very pleased to find that the three new catalysts **4a**–**c** could all be used to promote this Povarov reaction, delivering the corresponding 1,2,3,4-tetrahydroquinoline **9** as a single *cis*-diastereoisomer with moderate to good enantioselectivities (entries 4–6). All three catalysts derived from (*M*)-BINOL yielded the (2*S*,4*S*)-**9** as the major isomer. Given that the catalyst *ent*-**1** gave (2*R*,4*R*)-**9** as the major product, this result indicates that it is mainly the absolute configuration of the BINOL core that controls the stereochemistry of the reaction, as expected. The same holds true for the other catalytic reactions studied (see below). More in detail, the C_2-symmetric catalyst **4a**, with the methyl substituents pointing towards the phosphoric acid, was found to be the most efficient; its superior behavior compared with the 9-anthracenyl and 1-naphthyl derivatives **2** and **3** (entries 2 and 3) is remarkable, highlighting the importance of the steric hindrance furnished by these methyl substituents. However, even the other C_2-symmetric catalyst **4c**, with the methyl groups pointing outwards, was found to be superior to both **4b** (one methyl inwards, one methyl outwards) and the 9-anthracenyl catalyst **2**.

We then moved to study the related vinylogous Povarov reaction of the same aldimine **7** with 1-amidodiene **10** (Table 3).[17] According to our previous studies, this reaction is somehow complementary to the previous one in terms of catalyst requirements; catalyst **2** gives good enantioselectivity, whereas both the more hindered phosphoric acid **1** and the less substituted **3** afford very poor results (entries 1–3). The results reported in Table 3 with the new catalysts **4a**–**c** (entries 4–6) show that all these three structures performed much better than **1** and **3**, although the results obtained were lower than with the optimal **2**.

Table 3. Povarov reaction between imine **7** and 1-amidodiene **10** catalyzed by **4a**–**c**, and comparison with catalysts **1**–**3**.[a]

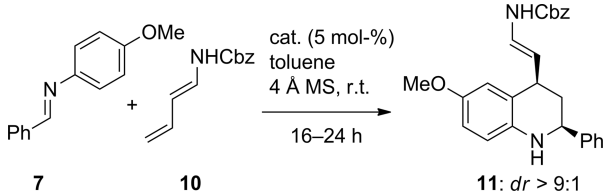

7 **10** **11**: *dr* > 9:1

Entry	Catalyst	Conversion [%][b]	*ee* [%][c]
1[d]	**1**	72	13
2[d]	**2**	59	92
3	**3**	60	32
4	**4a**	79	55
5	**4b**	83	67
6	**4c**	56	60
7[e]	**4b**	80	78

[a] Reaction conditions: imine **7** (0.025 mmol), catalyst **4** (0.00125 mmol, 5 mol-%), 1-amidodiene **10** (0.0375 mmol), 4 Å MS, toluene, room temp., 16–24 h. [b] Determined by ^{1}H NMR spectroscopic analysis after a plug on silica gel and evaporation of the solvents. [c] Determined by CSP-HPLC analysis. [d] Data taken from ref.[17] [e] Reaction performed at 0 °C.

As expected, catalyst **4c**, with the planar rings pointing inwards, gave better enantioselectivity than **4a** (methyl inwards). Somewhat surprisingly, in this case, the non-C_2-symmetric **4b** gave the best enantioselection among the set of catalysts **4**. The enantioinduction offered by this catalyst could be readily improved to a more satisfactory 78 % *ee* by cooling the reaction to 0 °C (entry 7).

Finally, we decided to test catalysts **4a**–**c** in the Friedel–Crafts addition of indole **13** to *N*-tosyl imine **12**.[21] In this reaction, unsubstituted 1-naphthyl groups at the 3,3′-positions of the BINOL core were reported to be optimal, catalyst **3** giving better results compared with **1** and **2** (Table 4, entries 1–3). Catalyst **3** has the same conformational features of **4a**–**c**, but the three diastereoisomers rapidly interconvert at ambient temperature, so the observed enantioselectivity is the result of a weighted average of the enantioselectivity of the three conformational diastereoisomers. Nevertheless, also for this reaction, catalysts **4a**–**c** performed rather well (entries 4–6), with the non-C_2-symmetric catalyst **4b** giving slightly better results than the two C_2-symmetric structures. Remarkably, all three catalysts furnished the product with respectable ee values of >80 %; furthermore, a reaction performed with catalyst **4a** at lower temperatures (–60 °C) showed that outstanding enantioselectivity in product **14** can be achieved (entry 7).

Table 4. Friedel–Crafts addition of indole **13** to *N*-tosylimine **12** catalyzed by **4a**–**c**, and comparison with catalysts **1**–**3**.[a]

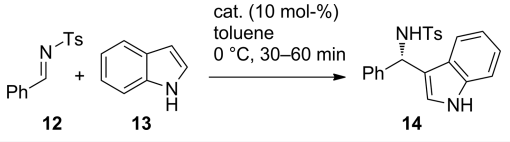

12 **13** **14**

Entry	Catalyst	Conversion[b] [%]	*ee*[c] [%]
1	**1**	83	52
2	**2**	89	30
3[d]	*ent*-**3**	80	95
4	**4a**	91	80
5	**4b**	89	86
6	**4c**	89	80
7[e]	**4a**	76	98

[a] Reaction conditions: imine **12** (0.025 mmol), catalyst **4** (0.0025 mmol, 10 mol-%), indole **13** (0.125 mmol), toluene, 0 °C, 30–60 min. [b] Determined by ^{1}H NMR spectroscopic analysis after a plug on silica gel and evaporation of the solvents. [c] Determined by CSP-HPLC analysis. [d] Refers to *ent*-**14**. Data taken from ref.[21a] [e] Reaction performed at –60 °C.

Conclusions

Three BINOL-derived phosphoric acids exhibiting atropisomerism in the 3,3′-positions were obtained by Suzuki coupling reaction of BINOL intermediates with 2-methylnaphthylboronic acid or 1-bromo-2-methylnaphthalene. The diastereomeric mixture was resolved by HPLC and the results of kinetic studies demonstrated that the coupling was stereoselective towards a C_2-symmetric diastereoisomer **4a**, whereas the equilibrium is shifted towards the C_1-symmetric diastereoisomer **4b**. Structural assignment was achieved by NOE-NMR spectroscopic analysis and by TD-DFT simulation of the ECD spectra.

The three atropisomeric phosphoric acids **4a**–**c** were tested in three enantioselective reactions (two Povarov cycloaddition reactions and a Friedel–Crafts addition of indole), comparing their ability to induce enantioselectivity with the related well-known structures **1**–**3** (Figure 1). The results obtained can be summarized as follows:

(1) All three catalysts **4a**–**c** of the set can be used to promote typical phosphoric acid catalyzed reactions of imines with moderate to good enantioselectivities; in one case, **4b** was found to be extremely efficient (98 % *ee*).
(2) A moderate influence of atropisomerism at the 3- and 3′-positions on the enantioinduction was observed. As expected, catalyst **4a**, featuring methyl groups pointing towards the active phosphoric acid, performed better in a reaction in which the highly hindered catalyst **1** had been previously found to be optimal. Instead, rather surprisingly, the non-C_2-symmetric structure **4b** (one methyl inward and one methyl outward) gave better results both in a reaction usually performed with 9-anthracenyl-substituted catalyst **2**, and in another transformation in which the 1-naphthyl derivative **3** was the most enantioselective structure.
(3) Whereas the results obtained with the previous optimal catalysts **1**–**3** in these reactions could not be reached by the new structures **4a**–**c**, it should be recognized that these new catalysts feature some intermediate properties, rendering them more "general" than structures **1**–**3**. In other words, they were able to afford moderately good results in all three reaction studied, whereas catalysts **1**–**3** were only competent in a single transformation.

Overall, the results demonstrate well the potential of atropisomeric conformational control at the 3,3′-position of the BINOL core in the rationalization of catalyst performances and in the design of new efficient structures.

Experimental Section

General Methods and Materials: *M*-2,2′-Dimethoxy-1,1′-binaphthalene and *M*-(2,2′-dimethoxy-[1,1′-binaphthalene]-3,3′-diyl)diboronic acid,[22] *M*-3,3′-diiodo-2,2′-dimethoxy-1,1′-binaphthalene[23] and 2-methylnaphthyl-boronic acid[24] were prepared as described previously. Silica gel 60 Å F254 (Merck) for the TLC and silica gel 60 Å (230–400 mesh, Sigma Aldrich) for atmospheric pressure chromatography were employed as stationary phases for the chromatography. Reactions that required anhydrous conditions were performed under a dry nitrogen flow. The glassware used in these reactions was placed in an oven at 100 °C for at least 3 h immediately before use. Semipreparative HPLC columns (Phenomenex C18 Kinetex® 250 × 20 mm, 5 μm) were used to purify the three diastereoisomers of **6**. Toluene was distilled from Na before use. *N*-4-Methoxyphenyl imine **7** was obtained by heating to reflux an equimolar mixture of 4-methoxyaniline and benzaldehyde in EtOH for 1–2 h, and collected by filtration. 2-Vinyl-1*H*-indole **8**,[25] *N*-Cbz 1-aminobutadiene **10**,[26] and *N*-tosylimine **12**[27] were prepared according to reported procedures. Racemic samples were prepared by using diphenylphosphoric acid as catalyst. The absolute configuration of the catalytic products **9**, **11**, and **14** was assigned by comparing their elution order on CSP-HPLC by using the same stationary phases and eluents as reported previously. The same enantiomer was obtained in the three tested reactions when using **4a**, **4b**, or **4c** as catalyst.

NMR spectra were recorded with a spectrometer operating at a field of 14.4 T (600 MHz for ^{1}H, 150.8 for ^{13}C) and at a field of 9.4 T (161.9 MHz for ^{31}P). Chemical shifts are given in ppm relative to the internal standard tetramethylsilane (^{1}H and ^{13}C). ^{31}P chemical shifts are given relative to the external standard 85 % H_3PO_4. The ^{13}C NMR spectra were acquired under proton decoupling conditions with a 36000 Hz spectral width, 5.5 μs (60° tip angle) pulse width, 1 s acquisition time, and 5 s delay time. A line broadening function of 1–2 Hz was applied before the Fourier transformation. The assignment of the ^{13}C NMR signals was achieved based on DEPT sequences. NOE spectra were obtained at 600 MHz by using the DPFGSE sequence[9] and a 50 Hz selective pulse with a R-SNOB shape.[28]

ECD spectra were recorded at 25 °C in far-UV HPLC-grade acetonitrile solutions. The concentrations of the samples (ca. 10^{-4} M) were tuned by dilution of a mother solution (1×10^{-3} M) to obtain a maximum absorbance of approximately 0.8–0.9 in the UV spectrum using a 0.2 cm path length. The spectra were recorded in the 190–400 nm interval as the sum of 16 spectra. Reported $\Delta\varepsilon$ values are expressed as L mol^{-1} cm^{-1}.

Ground-state optimizations and transition states were obtained by DFT computations performed by the Gaussian 09 rev. D.01 series of programs[29] using standard parameters. The calculations for ground states and transition states employed the B3LYP hybrid HF-DFT functional[30] and the 6-31G(d) basis set. The analysis of the vibrational frequencies for the optimized structures showed the absence of imaginary frequencies for the ground states, and the presence of one imaginary frequency for each transition state. Visual inspection of the corresponding normal mode validated the identification of the transition states. If not stated otherwise, the energy values presented in the results and discussion section derive from total electronic energies. The ECD spectra of *M*-BINOL and compounds **6a**–**c** were calculated by using TD-DFT with BH&HLYP, M06-2X, ωB97XD, CAM-B3LYP and the 6-311++G(2d,p) basis set. 70 discrete transitions were calculated for each conformation and the ECD spectrum was obtained by convolution of Gaussian shaped lines (0.5 eV line width). The simulated spectra resulting from the Boltzmann averaged sum of the conformations were redshifted by 6–12 nm to get the best simulations of the experimental spectra.

***M*-2,2′-Dimethoxy-3,3-di(2-methylnaphthyl)-1,1′-binaphthalene (5a–5c). Route A:** A mixture of *M*-(2,2′-dimethoxy-[1,1′-binaphthalene]-3,3′-diyl)-diboronic acid (0.5 g, 1.25 mmol), under nitrogen flux, were dissolved in a 3:1 mixture of dioxane/H_2O. Then $Ba(OH)_2 \cdot 8H_2O$ (2 g, 6.33 mmol), 1-bromo-2-metilnaphthalene (2.84 g mL, 12.83 mmol) and $Pd(PPh_3)_4$ (0.057 g, 4 % mol/mol) were added and the stirred solution was kept at 70 °C for 18–20 h. H_2O was then added and the solution was extracted three times with CH_2Cl_2. The organic layer was washed with 3 M HCl, dried (Na_2SO_4), filtered through silica gel and concentrated under reduced pressure. A pre-purification was achieved by chromatography on silica gel (*n*-hexane/ethyl acetate, 9:1), yielding 0.4 g (54 %) of a mixture of the three diastereoisomers **5a**–**c**, that was used in the following step.

Route B: A mixture of *M*-3,3′-diiodo-2,2′-dimethoxy-1,1′-binaphthalene (0.56 g, 1.0 mmol) and 2-methylnaphthylboronic acid (0.74 g 4.0 mmol), were dissolved in a 3:1 mixture of dioxane/H_2O under nitrogen flux. Then $Ba(OH)_2 \cdot 8H_2O$ (2 g, 6.33 mmol), and $Pd(PPh_3)_4$ (0.046 g, 4 % mol/mol) were added and the stirred solution was heated at 105 °C for 6 h. H_2O was then added and the solution was extracted three times with CH_2Cl_2. The organic layer was washed with 3 M HCl, dried (Na_2SO_4), filtered through silica gel and concentrated under reduced pressure. A pre-purification was achieved by chromatography on silica gel (*n*-hexane/ethyl acetate, 9:1), yielding 0.4 g (50 %) of a mixture of the three diastereoisomers **5a**–**c**, that was used in the following step.

***M*-3,3-Bis(2-methylnaphthyl)-1,1′-binaphthalene-2,2-diol (6a–c):** Prepared from *M*-2,2′-dimethoxy-3,3-di(2-methylnaphthyl)-1,1′-binaphthalene (**5a**–**c**) by following the procedure described previ-

ously.[22] The crude reaction mixture was pre-purified on silica gel (*n*-hexane/ethyl acetate, 8:2) yielding 304 mg of the diastereomeric mixture of **6a**–**c** (yield 80 %). The three diastereoisomers were than isolated by semipreparative HPLC on Phenomenex® Kinetex C18 column (250 × 20 mm, 5 µm; 20 mL/min; 254 nm UV detection; acetonitrile/H_2O, 85:15 v/v as eluent).

Compound 6a: Retention time: 16.25 min. ^{1}H NMR (600 MHz, CD_3CN, 25 °C): δ = 2.36 (s, 6 H), 6.19 (s, 2 H), 7.36–7.39 (m, 2 H), 7.39–7.45 (m, 4 H), 7.45–7.51 (m, 4 H), 7.54 (d, *J* = 8.3 Hz, 2 H), 7.57–7.61 (m, 2 H), 7.87 (s, 1 H), 7.92 (d, *J* = 8.3 Hz, 2 H), 7.93–7.96 (m, 4 H) ppm. ^{13}C NMR (150.8 MHz, CD_3CN, 25 °C): δ = 20.0 ($2C^3$), 114.1 (2Cq), 123.8 (2CH), 124.2 (2CH), 125.1 (2CH), 125.6 (2CH), 126.3$_5$ (2CH), 126.9 (2CH), 127.9 (2CH), 128.0 (2CH), 128.2 (2CH), 128.8 (2CH), 128.9 ($2C_q$), 129.6 ($2C_q$), 131.5 (2CH), 132.3 ($2C_q$), 133.3 ($2C_q$), 133.8 ($2C_q$), 134.2 ($2C_q$), 135.0 ($2C_q$), 151.8 ($2C_q$) ppm. HRMS (ESI-Orbitrap M-H): *m/z* calcd. for $C_{42}H_{29}O_2$: 565.2173; found 565.2171.

Compound 6b: Retention time: 17.05 min. ^{1}H NMR (600 MHz, CD_3CN, 25 °C): δ = 2.33 (s, 3 H), 2.40 (s, 3 H), 6.23 (s, 1 H), 6.25 (s, 1 H), 7.27–7.30 (m, 1 H), 7.34–7.43 (m, 6 H), 7.43–7.47 (m, 1 H), 7.47–7.50 (m, 2 H), 7.53 (d, *J* = 8.6 Hz, 1 H), 7.56 (d, *J* = 8.4 Hz, 1 H), 7.58–7.61 (m, 1 H), 7.67 (d, *J* = 8.6 Hz, 1 H), 7.87 (s, 2 H), 7.90–7.96 (m, 6 H) ppm. ^{13}C NMR (150.8 MHz, CD_3CN, 25 °C): δ = 20.0 ($1C^3$), 30.0 ($1C^3$), 114.0 ($1C_q$), 114.1 ($1C_q$), 123.8 (1CH), 123.8 (1CH), 124.1 (1CH), 124.2 (1CH), 125.1 (2CH), 125.6$_5$ (1CH), 125.9 (1CH), 126.1 (1CH), 126.3$_5$ (1CH), 126.9 (1CH), 127.0 (1CH), 127.8 (1CH), 127.9 (1CH), 127.9 (1CH), 128.0 (1CH), 128.2$_5$ (1CH), 128.3 (1CH), 128.8 (1CH), 128.8 (1CH), 128.9 ($1C_q$), 128.9 ($1C_q$), 129.6 ($1C_q$), 129.6 ($1C_q$), 131.5 (1CH), 131.5 (1CH), 132.3 ($1C_q$), 132.3 ($1C_q$), 133.3 ($2C_q$), 133.9 ($2C_q$), 134.1$_5$ ($1C_q$), 134.2 ($1C_q$), 134.9 ($1C_q$), 135.0 ($1C_q$), 151.8 ($1C_q$), 151.9 ($1C_q$) ppm. HRMS (ESI-Orbitrap, M-H): *m/z* calcd. for $C_{42}H_{29}O_2$: 565.2173; found 565.2170.

Compound 6c: Retention time: 17.75 min. ^{1}H NMR (600 MHz, CD_3CN, 25 °C): δ = 2.41 (s, 6 H), 6.26 (s, 2 H), 7.27–7.34 (m, 4 H), 7.37–7.45 (m, 6 H), 7.57 (d, *J* = 8.4 Hz, 2 H_{Ar}), 7.64 (d, *J* = 8.4 Hz, 2 H), 7.87 (s, 2 H), 7.90–7.96 (m, 6 H) ppm. ^{13}C NMR (150.8 MHz, CD_3CN, 25 °C): δ = 20.0 ($2CH_3$), 114.0 ($2C_q$), 123.8 (2CH), 124.0 (2CH), 125.0$_5$ (2CH), 125.9 (2CH), 126.1 (2CH), 127.0 (2CH), 127.8$_5$ (2CH), 127.9 (2CH), 128.3 (2CH), 128.8 (2CH), 128.9$_5$ ($2C_q$), 129.6 ($2C_q$), 131.5 (2CH), 132.3 ($2C_q$), 133.3 ($2C_q$), 134.0 ($2C_q$), 134.1 ($2C_q$), 134.9 ($2C_q$), 151.9 ($2C_q$) ppm. HRMS (ESI-Orbitrap, M-H): *m/z* calcd. for $C_{42}H_{29}O_2$: 565.2173; found 565.2169.

General Procedure for the Preparation of 4a–c:[18] To compound **6a**–**c** (20 mg, 1 equiv., 0.035 mmol) dissolved in anhydrous pyridine, $POCl_3$ (3.4 M in pyridine, 0.16 mL, 0.54 mmol, 15 equiv.) was slowly added under a positive nitrogen flux. The stirred mixture was kept at 60 °C until disappearance of the starting compound (16–20 h), then H_2O (1 mL) was added and the mixture was stirred and heated at 60 °C for an additional 3 h. HCl (3 M, 1 mL) was then added to the cooled solution and stirring was continued for 3 h. The mixture was diluted with CH_2Cl_2, washed with HCl (3 M, 3 × 20 mL) and then dried on Na_2SO_4. The crude material was purified on silica gel (CH_2Cl_2 then gradient to CH_2Cl_2/CH_3OH, 9:1) to give compound **4a**–**c** (yields 70–80 %). Spectroscopic characterization was performed after stirring the pure compound in 3 M HCl for 1 h followed by extraction with CH_2Cl_2 and drying on Na_2SO_4.

Compound 4a: ^{1}H NMR (600 MHz, $CDCl_3$, 25 °C): δ = 2.11 (s, 6 H), 6.96 (d, *J* = 7.9 Hz, 2 H_{Ar}), 7.22–7.29 (m, 4 H_{Ar}), 7.31–7.38 (m, 4 H_{Ar}), 7.41–7.45 (m, 2 H_{Ar}), 7.53–7.60 (m, 4 H_{Ar}), 7.75 (d, *J* = 8.0 Hz, 2 H_{Ar}), 7.87 (s, 2 H_{Ar}), 7.94 (d, *J* = 8.2 Hz, 2 H_{Ar}) ppm. ^{13}C NMR (150.8 MHz, $CDCl_3$, 25 °C): δ = 21.0 ($1CH_3$), 29.7 ($1CH_3$), 122.2 (d, $^3J_{13C-31P}$ = 2.3 Hz, $2C_q$), 124.6 (2CH), 125.4$_5$ (2CH), 125.9 (2CH), 126.1 (2CH), 126.6 (2CH), 127.4 (2CH), 127.7 (2CH), 127.8 (2CH), 128.3 (2CH), 129.1$_5$ (2CH), 131.4 ($2C_q$), 131.6 ($2C_q$), 131.7 (d$^3J_{13C-31P}$ = 3.3 Hz, $2C_q$,), 132.3 ($2C_q$), 132.3$_5$ ($2C_q$), 132.6 ($2C_q$), 132.7 (2CH), 135.3 ($2C_q$), 145.9 (d, $2C_q$, $^2J_{13C-31P}$ = 9.6 Hz) ppm. ^{31}P NMR (161.9 MHz, $CDCl_3$, 25 °C): δ = 2.40 (bs) ppm.

Compound 4b: ^{1}H NMR (600 MHz, $CDCl_3$, 25 °C): δ = 1.95 (s, 3 H), 2.18 (s, 3 H), 6.93 (d, *J* = 8.3 Hz, 1 H_{Ar}), 7.08 (d, *J* = 8.4 Hz, 1 H_{Ar}), 7.17 (t, *J* = 7.8 Hz, 1 H_{Ar}), 7.22 (t, *J* = 7.3 Hz, 2 H_{Ar}), 7.27 (d, *J* = 8.5 Hz, 1 H_{Ar}), 7.31 (t, *J* = 7.3 Hz, 1 H_{Ar}), 7.37 (d, *J* = 8.4 Hz, 1 H_{Ar}), 7.41 (d, *J* = 8.5 Hz, 1 H_{Ar}), 7.42–7.48 (m, 3 H_{Ar}), 7.53–7.61 (m, 5 H_{Ar}), 7.68 (d, *J* = 8.2 Hz, 1 H_{Ar}), 7.86 (s, 1 H_{Ar}), 7.90 (s, 1 H_{Ar}), 7.94 (d, *J* = 7.8 Hz, 1 H_{Ar}), 7.99 (d, *J* = 8.3 Hz, 1 H_{Ar}) ppm. ^{13}C NMR (150.8 MHz, $CDCl_3$, 25 °C): δ = 21.1$_5$ ($1CH_3$), 29.7 ($1CH_3$), 122.2 (d, $^3J_{13C-31P}$ = 2.23 Hz, $1C_q$), 122.3 (d, $^3J_{13C-31P}$ = 2.2 Hz, $1C_q$), 124.25, 124.5, 125.3, 125.4, 125.8$_5$, 125.9, 126.1, 126.3$_5$, 126.5$_6$, 126.6$_1$, 127.2, 127.3, 127.4, 127.7$_4$, 127.7$_9$, 127.8$_6$, 127.9$_5$, 128.3, 128.5, 128.9, 131.3$_4$, 131.4$_6$, 131.5$_4$, 131.5$_6$, 131.6$_5$, 131.8$_7$, 131.9$_1$, 131.9$_3$, 132.1$_8$, 132.2$_2$, 132.3, 132.5, 132.7$_5$, 132.9$_5$, 134.5, 135.1, 145.7 (d, $^2J_{13C-31P}$ = 8.9 Hz, $1C_q$), 145.9 (d, $^2J_{13C-31P}$ = 8.9 Hz, $1C_q$) ppm. ^{31}P NMR (161.9 MHz, $CDCl_3$, 25 °C): δ = 2.20 (bs) ppm.

Compound 4c: ^{1}H NMR (600 MHz, $CDCl_3$, 25 °C): δ = 2.09 (s, 6 H), 7.14 (t, *J* = 7.5 Hz, 2 HAr), 7.19 (d, *J* = 8.5 Hz, 2 HAr), 7.41–7.28 (m, 6 HAr), 7.51–7.59 (m, 8 HAr), 7.88 (s, 2 HAr), 7.97 (d, *J* = 8.1 Hz, 2 HAr) ppm. ^{13}C NMR (150.8 MHz, $CDCl_3$, +25 °C): δ = 20.5 ($2C^3$), 122.4 (d, $^3J_{13C-31P}$ = 2.2 Hz, $2C_q$), 124.4 (2CH), 125.3$_5$ (2CH), 125.8 (2CH), 126.6 (2CH), 126.8 (2CH), 127.1 (2CH), 127.2 (2CH), 127.6$_5$ (2CH), 128.3 (2CH), 128.4 (2CH), 131.3$_5$ ($2C_q$), 131.7 (d$^3J_{13C-31P}$ = 2.7 Hz, $2C_q$,), 131.8 ($2C_q$), 132.1 ($2C_q$), 132.3 ($2C_q$), 132.7 (2CH), 132.9 ($2C_q$), 134.6$_5$ ($2C_q$), 145.9$_5$ (d, $^2J_{13C-31P}$ = 9.1 Hz, $2C_q$) ppm. ^{31}P NMR (161.9 MHz, $CDCl_3$, 25 °C): δ = 2.07 (bs) ppm.

(2*S*,4*S*)-4-(1*H*-Indol-2-yl)-6-methoxy-2-phenyl-1,2,3,4-tetrahydroquinoline (9):[19a] To a flame-dried Schlenk tube equipped with a magnetic stirring bar, 3 Å spherical-shaped molecular sieves (ca. 70 mg) were added under a N_2 atmosphere. The molecular sieves were thermally activated under vacuum for 10 min and then cooled to room temp. The Schlenk tube was backfilled with N_2, then aldimine **7** (5.3 mg, 0.025 mmol) was added, followed by catalyst **4** (1.5 mg, 0.0025 mmol, 10 mol-%) and anhydrous toluene (0.5 mL). After heating to 45 °C, 2-vinylindole **8** (3.9 mg, 0.0275 mmol) was added. The mixture was then stirred at the same temperature under a N_2 atmosphere. After 3 h, the reaction mixture was diluted with CH_2Cl_2 and filtered through a plug of silica gel, and the plug was washed with EtOAc (4 ×). After concentration of the solvents, the residue was analyzed by ^{1}H NMR spectroscopy to determine the conversion of the reaction and the diastereomeric ratio of the cycloadduct **9** (>9:1 in all cases). ^{1}H NMR (300 MHz, $CDCl_3$, 25 °C): δ = 2.31 (br. q, *J* = 11.7 Hz, 1 H), 2.41 (ddd, *J* = 13.2, 6.2, 2.7 Hz, 1 H), 3.59 (s, 3 H), 6.59 (br. s, 1 H), 6.67–6.72 (m, 1 H), 7.07–7.16 (m, 2 H), 7.22–7.26 (m, 1 H), 7.28–7.35 (m 1 H), 7.35–7.41 (m, 2 H), 7.44–7.49 (m, 2 H), 7.55–7.60 (m, 1 H), 7.89 (br. s, 1 H) ppm. CSP-HPLC (Daicel Chiralcel® OD; *n*-hexane/isopropane, 80:20 v/v; 1 mL/min; room temp.): t_R = 15.9 (major), 18.9 (minor) min.

Benzyl {(*E*)-2-[(2*S*,4*R*)-6-Methoxy-2-phenyl-1,2,3,4-tetrahydroquinolin-4-yl]vinyl}carbamate (11):[17] To a flame-dried Schlenk tube equipped with a magnetic stirring bar, 4 Å powdered molecular sieves (ca. 20 mg) were added under a N_2 atmosphere. The molecular sieves were thermally activated under vacuum for 5 min and then cooled to room temp. After backfilling the Schlenk tube with N_2, aldimine **7** (5.3 mg, 0.025 mmol), catalyst **8** (0.8 mg, 0.00125 mmol, 5 mol-%), and toluene (100 µL) were added. The mixture was stirred for 5 min, then diene **10** (7.6 mg, 0.0375 mmol) was added. The mixture was stirred at room temp. under a N_2 at-

mosphere. After 16–24 h, the reaction mixture was diluted with CH_2Cl_2, filtered through a plug of silica gel, and the plug was washed with Et_2O (4 ×). After concentration of solvents, the residue was analyzed by ^1H NMR spectroscopy to determine the conversion of the reaction and diastereomeric ratio of the cycloadduct **11** (>9:1 in all cases). Finally, the product **11** was purified by chromatography on silica gel (petroleum ether/EtOAc, 9:1). ^1H NMR (600 MHz, $CDCl_3$, 25 °C): δ = 1.86 (q, J = 14.1 Hz, 1 H), 2.14–2.04 (m, 1 H), 3.68–3.59 (m, 1 H), 3.73 (s, 3 H), 3.80 (br. s, 1 H), 4.41 (d, J = 11.4 Hz,1 H), 4.90 (dd, J = 14.6, 10.3 Hz, 1 H), 5.15 (d, J = 12.8 Hz, 1 H), 5.18 (d, J = 12.8 Hz, 1 H), 6.50 (d, J = 9.1 Hz, 1 H), 6.54 (d, J = 10.1 Hz, 1 H), 6.65 (dd, J = 8.4, 2.9 Hz, 1 H), 6.76–6.68 (m, 2 H), 7.44–7.28 (m, 10 H) ppm. CSP-HPLC (Phenomenex Lux® Cellulose-1; *n*-hexane/*i*PrOH, 70:30; 0.75 mL/min; room temp.): t_R = 19.4 (major), 45.1 (minor) min.

(*S*)-*N*-[(1*H*-Indol-3-yl)(phenyl)methyl]-4-methylbenzenesulfonamide (14):[21] In a flame-dried Schlenk tube equipped with a magnetic stirring bar, imine **12** (6.5 mg, 0.025 mmol) and catalyst **4** (1.5 mg, 0.0025 mmol, 10 mol-%) were dissolved in anhydrous toluene (100 µL) under a N_2 atmosphere. After cooling the solution to 0 °C, indole **13** (15.0 mg, 0.125 mmol) was added. The reaction mixture was stirred for 30–60 min at the same temperature under N_2, then diluted with CH_2Cl_2, and filtered through a plug of silica gel. The plug was washed with EtOAc, and the solvent evaporated. The residue was analyzed by ^1H NMR spectroscopy to determine the conversion of the reaction. ^1H NMR (300 MHz, $CDCl_3$, 25 °C): δ = 2.34 (s, 3 H), 5.24 (d, J = 7.2 Hz, 1 H), 5.82 (d, J = 6.9 Hz, 1 H), 6.61 (d, J = 2.4 Hz, 1 H), 6.97 (t, J = 7.8 Hz, 1 H), 7.06 (d, J = 7.8 Hz, 2 H), 7.11–7.27 (m, 8 H), 7.53 (d, J = 8.4 Hz, 2 H), 8.02 (br., 1 H) ppm. CSP-HPLC (Daicel Chiralcel® OD; *n*-hexane/2-propanol, 80:20 v/v; 1 mL/min; λ = 254 nm; room temp.): t_R = 27 (major), 16 (minor) min.

Acknowledgments

The University of Bologna (RFO funds 2013) is gratefully acknowledged for financial support. ALCHEMY Fine Chemicals & Research (Bologna, www.alchemy.it) is acknowledged for a generous gift of chemicals.

Keywords: Organocatalysis · Enantioselectivity · Atropisomerism · Density functional calculations

[1] Reviews: a) D. Kampen, C. M. Reisinger, B. List, in: *Topics in Current Chemistry*, vol. 291: *Asymmetric Organocatalysis* (Ed.: B. List), Springer-Verlag, Heidelberg, Germany, **2010**, p. 395–456; b) T. Akiyama, *Chem. Rev.* **2007**, *107*, 5744; c) M. Terada, *Synthesis* **2010**, 1929; d) J. Yu, F. Shi, L.-Z. Gong, *Acc. Chem. Res.* **2011**, *44*, 1156; e) A. Zamfir, S. Schenker, M. Freund, S. B. Tsogoeva, *Org. Biomol. Chem.* **2010**, *8*, 5262; f) D. Parmar, E. Sugiono, S. Raja, M. Rueping, *Chem. Rev.* **2014**, *114*, 9047; g) J.-H. Xie, D.-H. Bao, Q.-L. Zhou, *Synthesis* **2015**, *47*, 460.

[2] S. Hoffmann, A. M. Seayad, B. List, *Angew. Chem. Int. Ed.* **2005**, *44*, 7424; *Angew. Chem.* **2005**, *117*, 7590.

[3] D. Uraguchi, K. Sorimachi, M. Terada, *J. Am. Chem. Soc.* **2005**, *127*, 9360.

[4] M. Rueping, E. Sugiono, C. Azap, T. Theissmann, M. Bolte, *Org. Lett.* **2005**, *7*, 3781.

[5] For phosphoric acid catalysts featuring unusual or additional stereogenic axes, see: a) Q.-S. Guo, D.-M. Du, J. Xu, *Angew. Chem. Int. Ed.* **2008**, *47*, 759; *Angew. Chem.* **2008**, *120*, 771; b) T. Honjo, R. J. Phipps, V. Rauniyar, F. D. Toste, *Angew. Chem. Int. Ed.* **2012**, *51*, 9684; *Angew. Chem.* **2012**, *124*, 9822; c) N. Momiyama, T. Konno, Y. Furiya, T. Iwamoto, M. Terada, *J. Am. Chem. Soc.* **2011**, *133*, 19294.

[6] B. Testa, in: *Studies in Organic Chemistry*, vol 6: *Principles of Organic Stereochemistry* (Ed.: P. G. Gassman), Marcel Dekker Inc., New York, **1979**, p. 86–87.

[7] E. P. Kyba, G. W. Gokel, F. De Jong, K. Koga, L. R. Sousa, M. G. Siegel, L. Kaplan, D. Y. Sogah, D. J. Cram, *J. Org. Chem.* **1977**, *42*, 4173.

[8] For a review, see: P. Lloyd-Williams, E. Giralt, *Chem. Soc. Rev.* **2001**, *30*, 145.

[9] J. Stonehouse, P. Adell, J. Keeler, A. J. Shaka, *J. Am. Chem. Soc.* **1994**, *116*, 6037–6038.

[10] For reviews, see: a) G. Bringmann, T. Bruhn, K. Maksimenka, Y. Hemberger, *Eur. J. Org. Chem.* **2009**, 2717; b) G. Pescitelli, L. Di Bari, N. Berova, *Chem. Soc. Rev.* **2011**, *40*, 4603; c) A. Mazzanti, D. Casarini, *WIREs Comput. Mol. Sci.* **2012**, *2*, 613.

[11] Being non-chromophoric, different disposition of the OH groups do not modify the simulations to a large extent.

[12] In Gaussian 09 the BH&HLYP functional has the form: $0.5*E_X^{HF} + 0.5*E_X^{LSDA} + 0.5*\Delta E_X^{Becke88} + E_C^{LYP}$.

[13] Y. Zhao, D. G. Truhlar, *Theor. Chem. Acc.* **2008**, *120*, 215.

[14] J.-D. Chai, M. Head-Gordon, *Phys. Chem. Chem. Phys.* **2008**, *10*, 6615.

[15] T. Yanai, D. Tew, N. Handy, *Chem. Phys. Lett.* **2004**, *393*, 51.

[16] M. Klussmann, L. Ratjen, S. Hoffmann, V. Wakchaure, R. Goddard, B. List, *Synlett* **2010**, *14*, 2189.

[17] L. Caruana, M. Fochi, S. Ranieri, A. Mazzanti, L. Bernardi, *Chem. Commun.* **2013**, *49*, 880.

[18] K. Shen, X. Liu, Y. Cai, L. Lin, X. Feng, *Chem. Eur. J.* **2009**, *15*, 6008–6014.

[19] a) G. Bergonzini, L. Gramigna, A. Mazzanti, M. Fochi, L. Bernardi, A. Ricci, *Chem. Commun.* **2010**, *46*, 327; b) L. Bernardi, M. Comes-Franchini, M. Fochi, V. Leo, A. Mazzanti, A. Ricci, *Adv. Synth. Catal.* **2010**, *352*, 3399; c) S. Duce, F. Pesciaioli, L. Gramigna, L. Bernardi, A. Mazzanti, A. Ricci, G. Bartoli, G. Bencivenni, *Adv. Synth. Catal.* **2011**, *353*, 860; d) S. Romanini, E. Galletti, L. Caruana, A. Mazzanti, F. Himo, S. Santoro, M. Fochi, L. Bernardi, *Chem. Eur. J.* **2015**, *21*, 17578.

[20] a) For a review, see: M. Fochi, L. Caruana, L. Bernardi, *Synthesis* **2014**, *46*, 135; for recent examples, see: b) W. Dai, X.-L. Jiang, J.-Y. Tao, F. Shi, *J. Org. Chem.* **2016**, *81*, 185; c) H.-H. Zhang, X.-X. Sun, J. Liang, Y.-M. Wang, C.-C. Zhao, F. Shi, *Org. Biomol. Chem.* **2014**, *12*, 9539.

[21] a) Q. Kang, Z.-A. Zhao, S.-L. You, *J. Am. Chem. Soc.* **2007**, *129*, 1484; b) F. Xu, D. Huang, C. Han, W. Shen, X. Lin, Y. Wang, *J. Org. Chem.* **2010**, *75*, 8677; c) C.-H. Xing, Y.-X. Liao, J. Ng, Q.-S. Hu, *J. Org. Chem.* **2011**, *76*, 4125; d) L. Simón, J. M. Goodman, *J. Org. Chem.* **2010**, *75*, 589.

[22] F. Romanov-Michailidis, L. Guénée, A. Alexakis, *Angew. Chem. Int. Ed.* **2013**, *52*, 9266; *Angew. Chem.* **2013**, *125*, 9436.

[23] S. Saha, C. Schneider, *Chem. Eur. J.* **2015**, *21*, 2348–2352.

[24] L. Lunazzi, M. Mancinelli, A. Mazzanti, M. Pierini, *J. Org. Chem.* **2010**, *75*, 5927.

[25] J. Waser, B. Gaspar, H. Nambu, E. M. Carreira, *J. Am. Chem. Soc.* **2006**, *128*, 11693.

[26] P. J. Jessup, C. B. Petty, J. Ross, L. E. Overman, *Org. Synth.* **1988**, *6*, 95.

[27] F. Chemla, V. Hebbe, J.-F. Normant, *Synthesis* **2000**, 75.

[28] E. Kupče, J. Boyd, I. D. Campbell, *J. Magn. Reson., Ser. B* **1995**, *106*, 300.

[29] M. J. Frisch, G. W. Trucks, H. B. Schlegel, G. E. Scuseria, M. A. Robb, J. R. Cheeseman, G. Scalmani, V. Barone, B. Mennucci, G. A. Petersson, H. Nakatsuji, M. Caricato, X. Li, H. P. Hratchian, A. F. Izmaylov, J. Bloino, G. Zheng, J. L. Sonnenberg, M. Hada, M. Ehara, K. Toyota, R. Fukuda, J. Hasegawa, M. Ishida, T. Nakajima, Y. Honda, O. Kitao, H. Nakai, T. Vreven, J. A. Montgomery Jr., J. E. Peralta, F. Ogliaro, M. Bearpark, J. J. Heyd, E. Brothers, K. N. Kudin, V. N. Staroverov, R. Kobayashi, J. Normand, K. Raghavachari, A. Rendell, J. C. Burant, S. S. Iyengar, J. Tomasi, M. Cossi, N. Rega, J. M. Millam, M. Klene, J. E. Knox, J. B. Cross, V. Bakken, C. Adamo, J. Jaramillo, R. Gomperts, R. E. Stratmann, O. Yazyev, A. J. Austin, R. Cammi, C. Pomelli, J. W. Ochterski, R. L. Martin, K. Morokuma, V. G. Zakrzewski, G. A. Voth, P. Salvador, J. J. Dannenberg, S. Dapprich, A. D. Daniels, Ö. Farkas, J. B. Foresman, J. V. Ortiz, J. Cioslowski, D. J. Fox, *Gaussian 09*, revision D.01, Gaussian, Inc., Wallingford CT, **2009**.

[30] a) C. Lee, W. Yang, R. G. Parr, *Phys. Rev. B* **1988**, *37*, 785; b) A. D. Becke, *J. Chem. Phys.* **1993**, *98*, 5648; c) P. J. Stephens, F. J. Devlin, C. F. Chabalowski, M. J. Frisch, *J. Phys. Chem.* **1994**, *98*, 11623.

Received: March 11, 2016
Published Online: ■

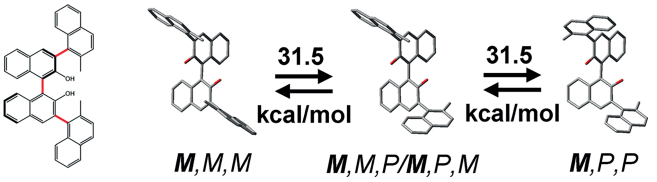

Three atropisomeric phosphoric acids for organocatalysis were obtained by a single Suzuki coupling reaction, and resolved by HPLC. All three catalysts could be used to promote organocatalytic reactions, rendering up to excellent enantioselectivity (98 % *ee*), confirming the potential of atropisomeric conformational control at the 3,3′-position of the BINOL core to infuence catalyst performance.

DOI: 10.1002/ejoc.201600296